

## Measurement of the spin polarization of the magnetic semiconductor EuS with zero-field and Zeeman-split Andreev reflection spectroscopy

Cong Ren,\* J. Trbovic, R. L. Kallaher, J. G. Braden, J. S. Parker, S. von Molnár, and P. Xiong†

Department of Physics and Center for Materials Research and Technology, Florida State University, Tallahassee, Florida 32306, USA

(Received 16 January 2007; published 29 May 2007)

We report measurements of the spin polarization ( $P$ ) of the concentrated magnetic semiconductor EuS using both zero-field and Zeeman-split Andreev reflection spectroscopy (ARS) with EuS/Al planar junctions. The zero-field ARS spectra are well described by the modified (spin-polarized) Blonder-Tinkham-Klapwijk (BTK) model with expected superconducting energy gap and actual measurement temperature (no additional spectral broadening). The fittings consistently yield  $P$  close to 80% regardless of the barrier strength. Moreover, we performed ARS in the presence of a Zeeman splitting of the quasiparticle density of states in Al. To describe the Zeeman-split ARS spectra, we develop a theoretical model which incorporates the solution to the Maki-Fulde equations into the modified BTK analysis. The method enables the determination of the magnitude as well as the sign of  $P$  with ARS, and the results are consistent with those from the zero-field ARS. The experiments extend the utility of field-split superconducting spectroscopy from tunnel junctions to Andreev junctions of arbitrary barrier strengths.

DOI: [10.1103/PhysRevB.75.205208](https://doi.org/10.1103/PhysRevB.75.205208)

PACS number(s): 72.25.Dc, 72.25.Mk, 74.45.+c

Superconducting spectroscopy has been one of the most effective means of determining the spin polarization ( $P$ ) of itinerant charge carriers in ferromagnetic materials. Two types of electron transport in a superconductor ( $S$ )/ferromagnet ( $Fm$ ) junction can be used for this purpose: single particle tunneling<sup>1</sup> and Andreev reflection (AR).<sup>2</sup> AR,<sup>3</sup> which occurs at an  $S$ /normal-metal ( $N$ ) interface, is a process that converts the quasiparticle current in  $N$  into supercurrent in  $S$ . In AR an incident electron from the  $N$  side pairs up with an electron of opposite spin and momentum to form a Cooper pair in order to enter the  $S$ , and a hole is retroreflected to conserve charge, spin, and momentum. Therefore, AR results in a doubling of charge transfer across the junction and an enhancement of the subgap junction conductance. In an  $S/Fm$  junction, AR is suppressed due to the spin imbalance near the Fermi level and the resulting reduction of the subgap Andreev conductance can in principle be used to infer  $P$ .<sup>4</sup> In practice, in most cases both AR and normal reflections are present and the zero-bias conductance alone does not give a reliable measure of  $P$ ; one needs to measure and analyze the entire conductance spectrum in order to separate the effects of spin polarization and single electron tunneling, and reliably determine  $P$ . The analysis of the conductance spectrum is done with a modified version of the Blonder-Tinkham-Klapwijk (BTK) theory,<sup>5</sup> which takes account of the spin polarization in the ferromagnet and computes the junction conductance with a two-current (spin polarized and unpolarized) model.<sup>6-8</sup> In the BTK theory the probability of AR and normal reflection is determined by the barrier strength, described by a dimensionless parameter  $Z$ , which includes effects of physical scattering as well as band structure mismatches. AR spectroscopy (ARS) has been widely implemented in point contact setups,<sup>4,8</sup> which has become an efficient technique for rapid measurement of  $P$  for a large variety of ferromagnetic materials in various forms. However, there remain several limitations and controversial issues with point contact ARS. First, a point contact typically does not represent an interface in a realistic device structure,

while the magnitude and even the sign of  $P$  is known to depend on the nature of the interface.<sup>9</sup> ARS, in general, only measures the magnitude of  $P$  and cannot determine its sign. Furthermore, the fitting of the point contact ARS often requires an artificially large spectral broadening<sup>10</sup> (or equivalently, the use of a temperature in the Fermi function much greater than the actual measurement temperature), and sometimes superconducting gaps much different from the expected values.<sup>8,10</sup> Finally, there are ubiquitous observations of a precipitous decline of measured  $P$  with increasing  $Z$  in a variety of systems,<sup>8,10-12</sup> which remain unexplained.

Single-particle tunneling in zero field cannot be used to measure  $P$  because of the degeneracy of the spin-up and spin-down electrons. However, the application of an external magnetic field lifts this degeneracy and the resulting asymmetry in the conductance spectrum can be utilized to calculate the magnitude and determine the sign of  $P$ .<sup>1</sup> Quantitative fits to the tunneling conductance spectrum with complex structures are realized by using the coupled spin-up and spin-down superconducting density of states (DOS) derived from the solution to the Maki-Fulde equations,<sup>13</sup> which produces highly reliable and unique  $P$  values.<sup>14,15</sup> Technically, such spin-polarized tunneling (SPT) experiments are more challenging to implement compared to ARS since they require fabrication of high-quality tunnel junctions and a superconducting electrode with high critical field and small spin-orbit coupling, which is in practice limited to an ultrathin Al film.

In this paper, we report on the zero-field and Zeeman-split ARS measurements of a series of doped-EuS/Al planar junctions. By controlling the growth temperature, the EuS films were naturally doped to different levels due to varying degree of sulfur vacancies,<sup>16</sup> which enabled realization of junctions of a relatively wide range of intermediate  $Z$  values where both AR and single electron tunneling are prominent. We observe that the conductance spectra can be fit straightforwardly (with zero additional spectral broadening and expected gap values) to the spin-polarized BTK model. The fittings consistently yield  $P$  of  $\sim 80\%$  regardless of the  $Z$

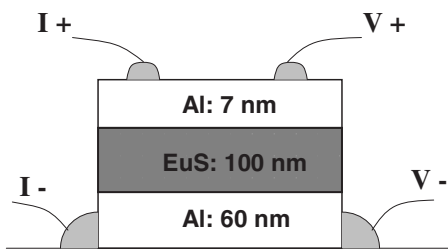


FIG. 1. A schematic diagram of the EuS/Al planar junction and the contact scheme. The numbers are the typical thicknesses of the films. The bottom junction of the thicker Al film and the EuS served as a low-resistance Ohmic contact to minimize current crowding.

values. Moreover, by using planar junctions and thin Al counterelectrode, we are able to obtain the ARS spectra in a large magnetic field. The Zeeman-split ARS experiments have provided a means to extract the sign of  $P$  from ARS. It also demonstrates that the field splitting of the conductance spectra is not limited to tunnel junctions but can be applied to  $S/Fm$  junctions of arbitrary barrier strengths, greatly simplifying its implementation. These experiments have provided a reliable determination of the magnitude ( $\sim 80\%$ ) and sign (+, majority spin polarized) of  $P$  for the doped EuS films.

EuS is a prototypical concentrated magnetic semiconductor. One of the most attractive features found in such materials is a strong exchange interaction between the spins of the itinerant charge carriers in the conduction band and the localized magnetic moments. This interaction is manifested as a giant spontaneous band splitting of  $\sim 0.5$  eV.<sup>17</sup> Such materials offer high magnetization and wide range of conductivity tunability so that they can be used as spin filters<sup>18,19</sup> in the insulating state and as spin injectors when doped.<sup>20–22</sup> Thus they offer an ideal system to demonstrate the physics of semiconductor-based spintronic devices in proof-of-concept studies.

Doped-EuS/Al planar junctions were fabricated by vacuum deposition on insulating Si(100) or glass (Corning) substrates. A schematic diagram of the junction structure is shown in Fig. 1. A relatively thick (50–60 nm) Al stripe was first deposited. Conducting EuS films of different conductivities, always 100 nm in thickness, were grown at various low substrate temperatures by electron beam evaporation in ultra-high vacuum. The growth temperature was shown to be effective in producing EuS films of varying doping levels, from intrinsic to degenerate, by controlling the degree of sulfur deficiency.<sup>16</sup> Finally, a thin Al electrode, 7–8 nm in thickness, was thermally deposited immediately over the EuS as a cross stripe defined by a shadow mask. The effective junction dimensions were  $0.4 \times 0.4$  mm<sup>2</sup>, and the junction resistances at liquid helium temperature varied from 3 to 15 k $\Omega$ . The conductance spectra were obtained in a <sup>3</sup>He system using standard phase-sensitive lock-in detection. The EuS films used in the present study had low-temperature resistivity on the order of m $\Omega$  cm and carrier density of  $\sim 10^{20}$  cm<sup>-3</sup>; they served as conducting electrodes rather than insulating tunnel barriers. The bottom Al/EuS junction made in this fashion always resulted in a low-resistance Ohmic contact, which served to ensure that there was negli-

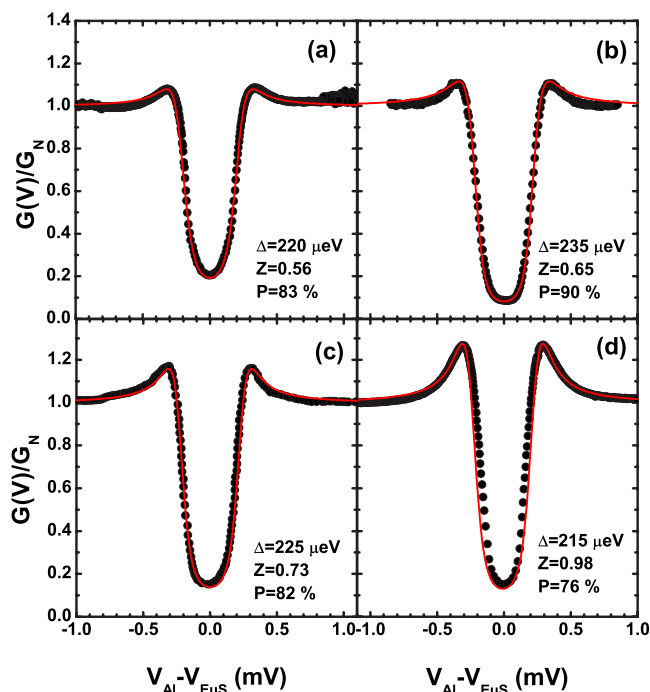


FIG. 2. (Color online) Normalized conductance versus bias voltage of the doped-EuS/Al junctions at a temperature of 0.38 K and zero magnetic field. The growth temperatures for EuS films are (a)  $-2$  °C; (b) 34 °C; (c) 80 °C; and (d) 120 °C. The solid lines are the best fits to the spin-polarized BTK theory. The fitting parameters are indicated in the figures.

gible current crowding in the top junction. A simple estimate of the resistance values shows that neither the EuS film nor the bottom contact contributes significantly to the measured resistance.<sup>23</sup> In addition, the application of a small parallel field of about 1 kG, which fully suppresses superconductivity in the thick bottom Al film but is much below the critical field of the thin top Al electrode (at least 1.8 T), had little effect on the conductance spectrum. This observation demonstrated unambiguously that the measured conductance spectra only reflected the top EuS/Al junction. The current ( $I$ )-voltage ( $V$ ) characteristics of the junction at temperatures above  $T_C$  of Al shows a linear behavior. This is in stark contrast to EuS/In junctions, which show a highly nonlinear  $I$ - $V$  characteristic of a Schottky barrier.<sup>23</sup>

Shown in Fig. 2 are the conductance spectra,  $dI/dV$  as a function of bias voltage  $V$ , for four EuS/Al junctions of different barrier strengths in zero magnetic field. Each spectrum is normalized by the corresponding one at a magnetic field above the critical field for the Al. Qualitatively these spectra are consistent with those of a  $S/Fm$  Andreev junction of intermediate  $Z$  and large  $P$  for the  $Fm$ , as judged from the much diminished quasiparticle peaks near the superconducting energy gap,  $\pm\Delta$ , and the low subgap conductance. These features are in contrast to the case of pure tunneling in EuS/In junctions where a Schottky barrier is present.<sup>23</sup> Quantitatively, these spectra can be analyzed within the spin-polarized BTK model. Excellent fits with physically sound parameters are obtained, as shown in Fig. 2. We emphasize that the fitting is always performed in a straightforward man-

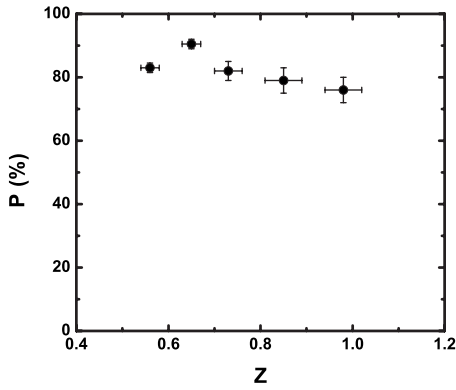


FIG. 3. The fitted  $P$  as a function of  $Z$  for various doped-EuS/Al junctions with different EuS growth temperatures.

ner and the only real adjustable fitting parameters are  $Z$  and  $P$ . First,  $T$  in all of the fits is always the actual measurement temperature; no additional spectral broadening, either in the form of an artificial  $T$  higher than the measurement temperature or an imaginary term in the electron energy,<sup>24</sup> is necessary to obtain good fits. This is evidence that Joule heating and inelastic effects including magnetic pairing-breaking are immeasurably small in these junctions. Second, the superconducting energy gaps for Al used are between 0.215 meV and 0.235 meV, values that are higher than that for bulk Al but expected of thin Al films.<sup>1</sup> The small variation in the gap value is most likely due to differences in the Al thickness. Third, the  $P$  values resulting from these measurements and fittings show no substantial decline with increasing  $Z$ , as shown in Fig. 3 in which we plot  $P$  from five such junctions as a function of  $Z$ . Within experimental uncertainty, there appears to be a small decrease of  $P$  with  $Z$ . However, this is in contrast to the results from point contact ARS in many systems where a much more significant decline of  $P$  (>50%) with  $Z$  was observed in a similar  $Z$  range.<sup>11</sup> We attribute the small decrease in  $P$  in our data to actual changes of  $P$  in films grown at increasing substrate temperatures (from  $-2$  °C to 120 °C), which is known to reduce the EuS film conductivity.<sup>16</sup> This result indicates that there is no intrinsic correlation between increase of spin-flip scattering and  $Z$  in these  $S/Fm$  junctions and a natural transition to the limit of SPT is possible. We point out that the above-described observations, including the straightforward excellent agreement with the spin-polarized BTK model and the insensitivity of the determined  $P$  with  $Z$ , are not limited to the EuS junctions. Similar results have been observed by us in junctions with the half-metal  $\text{CrO}_2$  (Ref. 25) and the ferromagnetic semimetal  $\text{EuB}_6$ .<sup>26</sup>

In the BTK model, the parameter  $Z$  includes physical (elastic) scattering at the  $S/N$  interface as well as effects of band structure mismatches. For example, the Fermi velocity mismatch results in an effective barrier strength given by<sup>27</sup>  $Z_{\text{eff}} = \sqrt{(1-r)^2/4r}$ , where  $r$  is the ratio of the Fermi velocities of the ferromagnet and superconductor. Under the present growth conditions, it is estimated that the EuS has a carrier (electron) density of  $\sim 2.0 \times 10^{20} \text{ cm}^{-3}$  at  $T=4.5 \text{ K}$ .<sup>16</sup> Assuming a parabolic band and a unitary effective electron mass, we estimate a Fermi velocity of  $v_F^{\text{EuS}} = 2.0 \times 10^5 \text{ m/s}$

compared to  $v_F^{\text{Al}} = 1.8 \times 10^6 \text{ m/s}$  for the superconducting electrode Al. Such a large mismatch should result in a substantial  $Z_{\text{eff}} = 1.35$  even in the absence of any physical scattering at the interface. The small  $Z$  values in our junctions can be qualitatively attributed to enhanced junction transparency due to a high spin polarization in the  $Fm$  electrode,<sup>28</sup> which has been widely observed in different  $S/Fm$  junctions of high  $P$ .<sup>25,29,30</sup> Another outstanding issue in our data is the magnitude of the junction resistance, which is several orders of magnitude higher than the prediction of the BTK theory (for a ballistic point contact). The discrepancy has been widely observed in  $S/\text{semiconductor}$  ( $Sm$ ) junctions of different materials and geometries.<sup>31–33</sup> Although a definitive explanation of this observation is still lacking, it is expected that the computation of the current and thus the junction resistance should depend on the junction geometry and be different in planar junctions.<sup>34</sup> It is important to note, however, that both in our junctions and other  $S/Sm$  structures<sup>31–33</sup> the conductance spectra are well described by the BTK theory. This represents a far more stringent requirement and strongly supports its applicability in these structures. This assertion is further reinforced by our results from measurements of the conductance spectra under Zeeman-splitting magnetic fields.

The use of a planar junction structure and thin Al electrodes afford us the opportunity to Zeeman split the superconducting DOS and examine its consequences on the ARS spectrum. Figure 4(a) shows the conductance curves of the EuS/Al junction of Fig. 2(a) at in-plane magnetic fields of 0.6 and 0.75 T. Because the Al electrode was on top of the EuS, it needed to be relatively thick (7–8 nm) which resulted in a relatively low critical field ( $< 2 \text{ T}$ ). However, even these relatively low magnetic fields induce a sizable shift of the conductance curve to the left-hand side. With the exception of noticeable asymmetry near the peaks, there are no observable additional features due to the minority spins. Qualitatively, these observations indicate a large, positive,  $P$  for the doped EuS. This experiment represents a study of Zeeman-split ARS in low- $Z$   $S/Fm$  junctions.

In order to analyze the Zeeman-split ARS spectrum and independently extract  $P$  from the analysis, a thorough treatment of spin-polarized charge transport in an Andreev junction with Zeeman splitting is necessary. This requires the use of the appropriate spin-resolved DOS for Al in a magnetic field when calculating the BTK transport (reflection and transmission) coefficients (Table II in Ref. 5). The BTK coefficients depend only on the parameter  $Z$  and the coherence factors

$$u_0^2 = 1 - v_0^2 = \frac{1}{2} \left( 1 + \frac{1}{N_S(E)} \right), \quad (1)$$

where  $N_S(E)$  is the normalized BCS DOS

$$N_S(E) = \frac{|E|}{\sqrt{E^2 - \Delta^2}}. \quad (2)$$

In a magnetic field  $N_S(E)$  is Zeeman split and the BTK coefficients consequently become spin-dependent. Melin<sup>35</sup> assumed a simple Zeeman splitting of the BCS DOS in an

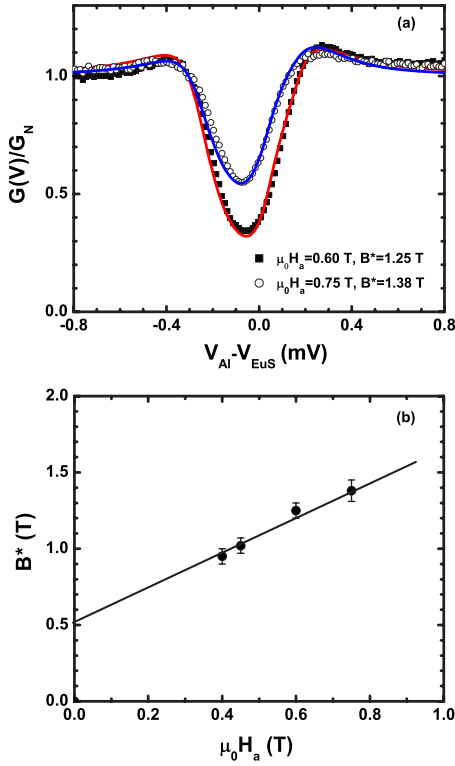


FIG. 4. (Color online) (a) The Zeeman-split conductance spectra for a doped-EuS/Al junction whose zero-field spectrum is shown in Fig. 2(b). The solid lines are the fits to the spin-polarized BTK theory that incorporates the solution to the Maki-Fulde equations; (b) The effective field  $B^*$  used in the fittings as a function of the applied field. The solid line is a linear fit to the data.

applied field and obtained the spin-dependent BTK coefficients using

$$u_{\uparrow(\downarrow)}^2 = 1 - v_{\uparrow(\downarrow)}^2 = \frac{1}{2} \left( 1 + \frac{\sqrt{(E \pm \mu_B H)^2 - \Delta^2}}{|E \pm \mu_B H|} \right), \quad (3)$$

where  $H$  is the applied magnetic field. The Zeeman-split conductance curves at 0 K were then computed. This approach neglects the effects of spin-orbit coupling and depairing from the applied field. It has been shown<sup>14,15</sup> that these effects are not negligible even in a material such as Al. They result in significant modification of the Zeeman-split conductance spectrum and, particularly, ambiguity in the determination of  $P$  from it. To obtain the DOS of a superconducting film in the presence of spin-orbit coupling (parameter  $b$ ) and pair-breaking due to a magnetic field (parameter  $\zeta$ , which is proportional to  $H^2$ ), one needs to solve the Maki-Fulde equations:

$$u_{\pm} = \frac{E \mp \mu_B H}{\Delta} + \frac{\zeta u_{\pm}}{\sqrt{1 - u_{\pm}^2}} + b \left( \frac{u_{\mp} - u_{\pm}}{\sqrt{1 - u_{\mp}^2}} \right). \quad (4)$$

The solution of the coupled equations enables the determination of the spin-resolved superconducting DOS,

$$\rho_{\uparrow(\downarrow)} = \frac{\rho(0)}{2} \operatorname{Im} \left( \frac{u_{\pm}}{\sqrt{1 - u_{\pm}^2}} \right), \quad (5)$$

where  $\rho_{\uparrow(\downarrow)}$  are the spin-up (down) superconducting DOS,  $\rho(0)$  is the normal state DOS of the superconductor at  $E_F$ . The spin-up (down) DOS can then be used to calculate the corresponding spin-resolved BTK coefficients

$$u_{\uparrow(\downarrow)}^2 = 1 - v_{\uparrow(\downarrow)}^2 = \frac{1}{2} \left( 1 + \frac{1}{N_{S\uparrow(\downarrow)}(E)} \right), \quad (6)$$

where

$$N_{S\uparrow(\downarrow)} = \operatorname{Im} \left( \frac{u_{\pm}}{\sqrt{1 - u_{\pm}^2}} \right). \quad (7)$$

We numerically solve the Maki-Fulde equations [Eq. (4)] and obtain the actual DOS of the Al film in a magnetic field. The results are similar to those obtained in Ref. 14 and used in the analysis of Al/*Fm* tunnel junctions ( $Z \gg 1$ ).<sup>14,15</sup> Using the DOS we obtain the spin-dependent coherence factors [Eq. (6)] and consequently the BTK coefficients for different transport processes at arbitrary barrier strength  $Z$ . We then calculate the junction conductance under Zeeman splitting using these coefficients and the two-current model.<sup>36</sup> This, therefore, is a general theoretical framework that contains BTK,<sup>5</sup> spin-polarized BTK,<sup>7,8</sup> and Meservey-Tedrow<sup>1</sup> analysis as special cases. It enables the quantitative analysis of the field-split conductance spectrum of *S/Fm* junctions of arbitrary barrier strength. As pointed out by Mazin,<sup>37</sup> ARS and spin-polarized tunneling in general probe different forms of spin polarization. In ARS, especially, depending on whether the electron transport at the junction interface is ballistic or diffusive, the spin densities are weighted differently by the Fermi velocities to produce different current spin polarization. Our junctions are clearly in the diffusive regime, and the measured  $P$  corresponds to a value with spin densities weighted by  $v_{F\uparrow(\downarrow)}^2$  [Eq. (2) of Ref. 37]. In Mazin's theory,<sup>37</sup>  $P$  takes the same form in the purely diffusive regime and when  $Z \gg 1$  (tunneling limit). Thus a natural crossover exists between our case and the Meservey-Tedrow regime.<sup>14,15</sup>

The solid lines in Fig. 4(a) are the best fits to the data using the above scheme. The fits yield  $P$  of 78% and 73% for applied fields ( $\mu_0 H_a$ ) of 0.6 T and 0.75 T, respectively. In the fits the following parameters are used:  $\zeta=0.10$ ,  $b=0.14$  and effective magnetic field  $B^*$  of 1.25 T and 1.38 T, respectively. The parameter  $Z$  (0.65) is determined independently from the zero-field data [Fig. 2(b)]. Although there are a number of parameters in the fitting, the complexity of the Zeeman-split conductance spectra makes the determination of the parameters highly unique and reliable. The necessity to use an effective magnetic field  $B^*$  greater than the applied field is readily apparent from the large shift of the conductance minimum from the zero bias. In Fig. 4(b) we plot  $B^*$  as a function of  $\mu_0 H_a$  (which are all greater than the saturation field of the EuS). A linear fit of the data results in an intercept of 0.52 T at  $\mu_0 H_a=0$ . These observations are consistent with the enhanced Zeeman splitting in junctions where the Al films were in direct contact with an insulating EuS barrier.<sup>18</sup>

This enhanced Zeeman splitting originates from the exchange interaction of EuS on Al due to the intimate contact between them in these junctions. This is to be contrasted with the case of tunnel junctions where the Al is separated from the ferromagnet by a nonmagnetic insulator.<sup>14</sup> This intimate contact also results in the large  $\zeta$  and  $b$  compared to those in pure Al, similar to the observation of much enhanced spin-orbit interaction in thin Al with heavy impurities such as rare earths<sup>38</sup> and noble metals<sup>1</sup> on the surface. The  $P$  determined from the fittings is close to the value from zero-field ARS on the same junction, but there appears to be a small but systematic decrease of the measured  $P$  with increasing magnetic field. This decrease in  $P$  is beyond the experimental uncertainty and remains an open question.

In summary, we have performed a set of experiments to determine the spin polarization of the magnetic semiconductor EuS using Andreev reflection spectroscopy. Zero-field ARS on a series of EuS/Al junctions of different barrier strengths consistently yielded conductance spectra that fit straightforwardly to the spin-polarized BTK model and  $P$  on the order of 80% for the naturally doped EuS, regardless of the barrier strength. Perhaps more importantly, we have for the first time realized ARS in a large Zeeman-splitting mag-

netic field in an  $S/Fm$  Andreev junction. The Zeeman-split ARS spectra are well described via a modification of the BTK model to incorporate the Al quasiparticle DOS in a magnetic field. The zero-field results provide strong evidence for the applicability of the spin-polarized BTK model to ARS in planar  $S/Fm$  junctions and the validity of its application for the determination of the spin polarization of magnetic semiconductors. The experimental realization of the Zeeman-split ARS and the development of a theoretical framework for its understanding in junctions of arbitrary barrier strength should greatly expand the utilization of the field-split superconducting spectroscopy for the measurement of the magnitude and sign of the spin polarization of ferromagnetic metals and semiconductors. The high  $P$  in the doped EuS films makes them an attractive source of spin-polarized electrons in proof-of-concept spintronics studies.

The authors thank P. Schlottmann for his contributions in the analysis of the Zeeman-split ARS and P. Stiles for helpful discussions. One of the authors (C.R.) would also like to thank Ian Winger and Dan Read for technical assistance. This work was supported by DARPA through ONR Grant Nos. N-00014-00-1094 and MDA-072-02-1-0002DARPA.

\*Present address: Laboratory for Superconductivity, Institute of Physics, Chinese Academy of Sciences, Beijing 100080.

<sup>†</sup>Electronic address: xiong@martech.fsu.edu

- <sup>1</sup>R. Meservey and P. M. Tedrow, *Phys. Rep.* **238**, 173 (1994).
- <sup>2</sup>M. J. M. de Jong and C. W. J. Beenakker, *Phys. Rev. Lett.* **74**, 1657 (1995).
- <sup>3</sup>A. F. Andreev, *Zh. Eksp. Teor. Fiz.* **46**, 1823 (1964) [*Sov. Phys. JETP* **19**, 1228 (1964)].
- <sup>4</sup>R. J. Soulen, J. M. Byers, M. S. Osofsky, B. Nadgorny, T. Ambrose, S. F. Cheng, P. R. Broussard, C. T. Tanaka, J. Nowak, J. S. Moodera, A. Barry, and J. M. D. Coey, *Science* **282**, 85 (1998).
- <sup>5</sup>G. E. Blonder, M. Tinkham, and T. M. Klapwijk, *Phys. Rev. B* **25**, 4515 (1982).
- <sup>6</sup>S. K. Upadhyay, A. Palanisami, R. N. Louie, and R. A. Buhrman, *Phys. Rev. Lett.* **81**, 3247 (1998).
- <sup>7</sup>I. I. Mazin, A. A. Golubov, and B. Nadgorny, *J. Appl. Phys.* **89**, 7576 (2001).
- <sup>8</sup>G. J. Strijkers, Y. Ji, F. Y. Yang, C. L. Chien, and J. M. Byers, *Phys. Rev. B* **63**, 104510 (2001).
- <sup>9</sup>J. M. de Teresa, A. Bartheley, A. Fert, J. P. Contour, F. Montaigne, and P. Seneor, *Science* **286**, 507 (1999).
- <sup>10</sup>Y. Bugoslavsky, Y. Miyoshi, S. K. Clowes, W. R. Branford, M. Lake, I. Brown, A. D. Caplin, and L. F. Cohen, *Phys. Rev. B* **71**, 104523 (2005).
- <sup>11</sup>G. T. Woods, R. J. Soulen, I. I. Mazin, B. Nadgorny, M. S. Osofsky, J. Sanders, H. Srikanth, W. F. Egelhoff, and R. Datla, *Phys. Rev. B* **70**, 054416 (2004).
- <sup>12</sup>C. H. Kant, O. Kurnosikov, A. T. Filip, P. LeClair, H. J. M. Swagten, and W. J. M. de Jonge, *Phys. Rev. B* **66**, 212403 (2002).
- <sup>13</sup>K. Maki, *Prog. Theor. Phys.* **31**, 731 (1964); K. Maki and P. Fulde, *Phys. Rev.* **140**, A1586 (1965).

- <sup>14</sup>D. C. Worledge and T. H. Geballe, *Phys. Rev. B* **62**, 447 (2000).
- <sup>15</sup>D. J. Monsma and S. S. P. Parkin, *Appl. Phys. Lett.* **77**, 720 (2000).
- <sup>16</sup>J. Keller, J. S. Parker, J. Stankiewicz, D. E. Read, P. A. Stampe, R. J. Kennedy, P. Xiong, and S. von Molnár, *IEEE Trans. Magn.* **38**, 2673 (2002); I. J. Guilaran, D. E. Read, R. L. Kallaher, P. Xiong, S. von Molnár, P. A. Stampe, R. J. Kennedy, and J. Keller, *Phys. Rev. B* **68**, 144424 (2003).
- <sup>17</sup>W. A. Thompson, T. Penney, F. Holtzberg, and S. Kirkpatrick, *Proceeding of the 11th International Conference on Physics of Semiconductors*, Warsaw, 1972, p. 1255.
- <sup>18</sup>J. S. Moodera, X. Hao, G. A. Gibson, and R. Meservey, *Phys. Rev. Lett.* **61**, 637 (1988); X. Hao, J. S. Moodera, and R. Meservey, *Phys. Rev. B* **42**, 8235 (1990).
- <sup>19</sup>P. LeClair, J. K. Ha, H. J. M. Swagten, J. T. Kohlhepp, C. H. van de Vin, and W. J. M. de Jonge, *Appl. Phys. Lett.* **80**, 625 (2002).
- <sup>20</sup>S. von Molnár and T. Kasuya, *Phys. Rev. Lett.* **21**, 1757 (1968).
- <sup>21</sup>N. Müller, W. Ecjstein, W. Heiland, and W. Zinn, *Phys. Rev. Lett.* **29**, 1651 (1972).
- <sup>22</sup>J. Trbovic, Cong Ren, P. Xiong, and S. von Molnár, *Appl. Phys. Lett.* **87**, 082101 (2005).
- <sup>23</sup>C. Ren, J. Trbovic, P. Xiong, and S. von Molnár, *Appl. Phys. Lett.* **86**, 012501 (2005).
- <sup>24</sup>R. C. Dynes, V. Narayanamurti, and J. P. Garno, *Phys. Rev. Lett.* **41**, 1509 (1978).
- <sup>25</sup>J. S. Parker, S. M. Watts, P. G. Ivanov, and P. Xiong, *Phys. Rev. Lett.* **88**, 196601 (2002).
- <sup>26</sup>X. Zhang, S. von Molnár, P. Xiong, and Z. Fisk (unpublished).
- <sup>27</sup>G. E. Blonder and M. Tinkham, *Phys. Rev. B* **27**, 112 (1983).
- <sup>28</sup>Igor Žutić and S. Das Sarma, *Phys. Rev. B* **60**, R16322 (1999).
- <sup>29</sup>Y. Ji, G. J. Strijkers, F. Y. Yang, C. L. Chien, J. M. Byers, A. Anguelouch, G. Xiao, and A. Gupta, *Phys. Rev. Lett.* **86**, 5585

- (2001).
- <sup>30</sup>J. G. Braden, J. S. Parker, P. Xiong, S. H. Chun, and N. Samarth, *Phys. Rev. Lett.* **91**, 056602 (2003).
- <sup>31</sup>W. M. van Hufelen, T. M. Klapwijk, D. R. Heslinga, M. J. de Boer, and N. van der Post, *Phys. Rev. B* **47**, 5170 (1993).
- <sup>32</sup>J. R. Gao, J. P. Heida, B. J. van Wees, S. Bakker, T. M. Klapwijk, and B. W. Alphenaar, *Appl. Phys. Lett.* **63**, 334 (1993).
- <sup>33</sup>S. De Franceschi, F. Giazotto, F. Beltram, L. Sorba, M. Lazzarino, and A. Franciosi, *Appl. Phys. Lett.* **73**, 3890 (1998).
- <sup>34</sup>C. W. J. Beenakker, *Rev. Mod. Phys.* **69**, 731 (1997).
- <sup>35</sup>R. Melin, *Europhys. Lett.* **51**, 202 (2000).
- <sup>36</sup>P. Schlottmann (unpublished).
- <sup>37</sup>I. I. Mazin, *Phys. Rev. Lett.* **83**, 1427 (1999).
- <sup>38</sup>P. M. Tedrow, J. E. Tkaczyk, and A. Kumar, *Phys. Rev. Lett.* **56**, 1746 (1986); J. E. Tkaczyk and P. M. Tedrow, *J. Appl. Phys.* **61**, 3368 (1987).